

ARTICLE TYPE

Nonparametric Regression and Error Covariance Function Estimation - Beyond Short-Range Dependence

Sisheng Liu¹ | Xiaoli Kong²

¹MOE-LCSM, School of Mathematics and Statistics, Hunan Normal University, Changsha, China

²Department of Mathematics, Wayne State University, Detroit, MI, USA

Correspondence

Corresponding author Sisheng Liu, MOE-LCSM, School of Mathematics and Statistics, Hunan Normal University, Changsha, Hunan 410081, P. R. China.

Email: ssl1989@hunnu.edu.cn

Present address

ssl1989@hunnu.edu.cn

Abstract

In nonparametric regression analysis, errors are possibly correlated in practice, and neglecting error correlation can undermine most bandwidth selection methods. When no prior knowledge or parametric form of the correlation structure is available in the random design setting, this issue has primarily been studied in the context of short-range dependent errors. When the data exhibits correlations that decay much more slowly, we introduce a special class of kernel functions and propose a procedure for selecting bandwidth in kernel-based nonparametric regression, using local linear regression as an example. Additionally, we provide a nonparametric estimate of the error covariance function, supported by theoretical results. Our simulations demonstrate significant improvements in estimating the nonparametric regression and error covariance functions, particularly in scenarios beyond short-range dependence. The practical application of our procedure is illustrated through the analysis of three datasets: cardiovascular disease mortality, life expectancy, and colon and rectum cancer mortality in the Southeastern United States.

KEY WORDS

Nonparametric regression, Correlated errors, Bandwidth, Covariance estimation, Short-range, Disease mapping

1 | INTRODUCTION

Assume that we observe random samples (\mathbf{X}_i, Y_i) for $i = 1, \dots, n$, where Y_i takes values in \mathbb{R} and $\mathbf{X}_i = (X_{i1}, \dots, X_{iD})^T$ takes values in $\mathcal{X} \subset \mathbb{R}^D$ with a common probability density f . The density f is compactly supported, bounded and continuous with $f(\mathbf{x}) > 0$ for all $\mathbf{x} \in \mathcal{X}$. Consider the model:

$$Y_i = \mu(\mathbf{X}_i) + \varepsilon_i, \quad \text{for } i = 1, \dots, n, \quad (1)$$

where μ is an unknown smooth (at least twice continuously differentiable) regression function and the ε_i 's are unobserved random errors such that

$$E(\varepsilon_i | \mathbf{X}_i) = 0, \quad \text{Cov}(\varepsilon_i, \varepsilon_j | \mathbf{X}_i, \mathbf{X}_j) = \sigma^2 \rho_n(\|\mathbf{X}_i - \mathbf{X}_j\|), \quad \text{for } i, j \in \{1, \dots, n\},$$

with $\sigma^2 < \infty$ and ρ_n a stationary correlation function satisfying $\rho_n(0) = 1$ and $|\rho_n(\|\mathbf{x}_i - \mathbf{x}_j\|)| \leq 1$ for all $\mathbf{x}_i, \mathbf{x}_j \in \mathcal{X}$.

Kernel-based nonparametric regression methods usually require an appropriate bandwidth to estimate the regression function. However, bandwidth selection methods developed under the assumption of independent and identically distributed (i.i.d.) errors tend to break down in the presence of correlated errors. This problem has been widely studied, see the review paper of Opsomer et al.¹. When prior knowledge or parametric form of the correlation structure is available or assumed, many bandwidth selection methods have been developed, for example, difference-based time series cross-validation², plug-in bandwidth selection for AR(1) error process³, modified generalized cross-validation method for spatial data⁴, far casting cross-validation⁵ and generalised correlated cross-validation⁶, etc.

Abbreviations: ANA, anti-nuclear antibodies; APC, antigen-presenting cells; IRF, interferon regulatory factor.

There are a few methods that have been developed to bypass the estimation of the error correlation structure. Most of them are based on a bimodal kernel function to mitigate the effect of error correlation e.g.^{7,8}. These methods are restricted to one-dimensional, equal-distance, fixed designs. Brabanter et al⁹ first applied the bimodal kernel to remove the error correlation structures in local polynomial regression with random design. Recently, Liu and Yang¹⁰ and Kong et al¹¹ adopted the bimodal kernel for both nonparametric regression function and derivative estimation. Although the bimodal kernel can mitigate the impact of error correlation on bandwidth selection, it is effective only for short-range dependence.

The major motivation of our article comes from the Global Health Data Exchange, which records a variety of disease data by different counties in the United States (and also other countries). These data sets can be useful for analyzing the spatial distribution of various type of disease for the interests of the epidemiologist, including the Cardiovascular Mortality Rates data, the Life Expectancy Data, the Cancer Mortality Rates data etc. All these datasets conform to model (1), where the two-dimensional random vector \mathbf{X}_i represents the latitude and longitude of each county. Figure 1(a) illustrates the Cardiovascular Mortality Rates in the Southeastern United States at the year 2014, displaying a clear nonlinear trend in mortality rates, which indicate that a nonparametric fit would be appropriate. In addition, we applied local linear regression with bandwidth chosen via generalized cross-validation and then used the residuals to compute the empirical error covariance. Figure 1(b) plots the empirical error covariance against the distances, revealing that errors may exhibit strong dependence. In Section 5, we will demonstrate that the bimodal kernel function fails to mitigate the impact of error correlation on bandwidth selection in the motivated example. Moreover, another two data examples — the Life Expectancy and the Colon & Rectum cancer mortality rate, will be present in the Supplementary file.

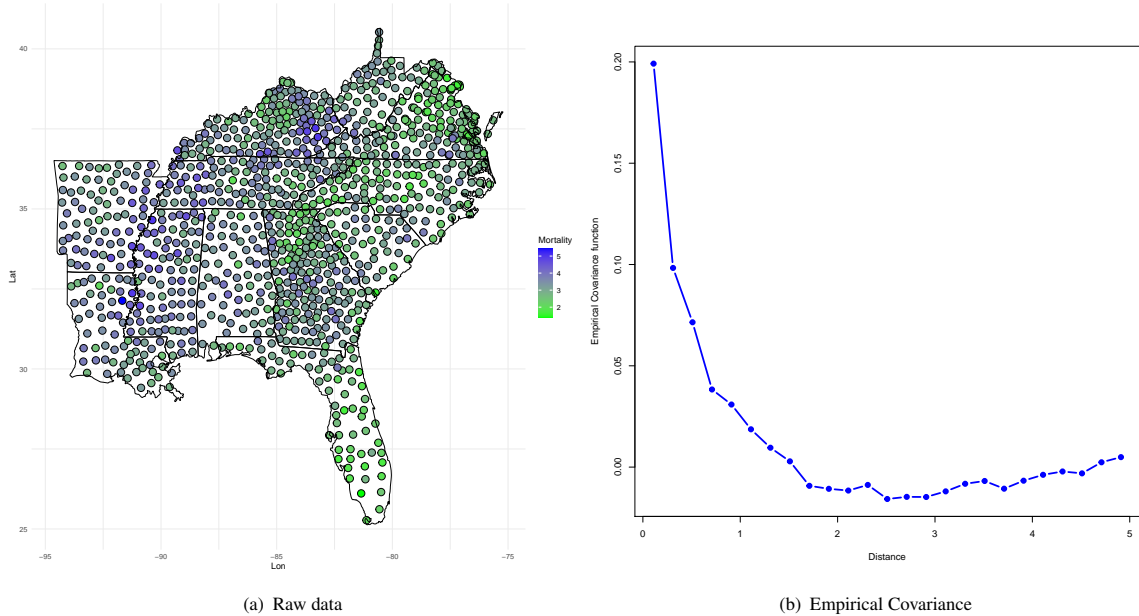


FIGURE 1 The left panel is the cardiovascular disease mortality rates of 1064 counties in the southeastern United States in the year 2014. The right panel is the empirical covariance versus the distance ($\times 10^2$ km).

In this paper, we introduce a new class of kernel functions and propose a procedure for selecting bandwidth in kernel-based regression. We use local linear regression as an example. Under mild conditions, it is shown that the selected bandwidth is asymptotically optimal in the sense of minimizing the Mean Integrated Square Error. The proposed selection procedure performs better for more complex correlation structures and remains effective for short-range dependent errors.

While the proposed bandwidth selection procedure does not require knowing the correlation structure, the estimation of the error covariance function has numerous potential applications, including but not limited to its use in kernel ridge regression with incorporated error covariance¹², tuning parameter selection in derivative estimation¹³, and in real data applications where the correlation structure reflects relationships among various observed times/locations, such as our motivated examples. However,

most nonparametric estimations of the error covariance function rely on assumptions of fixed equally spaced designs, m -dependence, strong mixing with exponential decay rate, auto-regression^{2 14–18}. In random design settings, the methods proposed by Hall et al¹⁹ and Choi et al²⁰, do not assume a nonparametric form of the regression function.

Our second contribution in this paper is the development of nonparametric estimations for the error covariance function in random design using kernel smoothing. We investigate the theoretical properties of the estimation without assuming any covariance structure. Our proposed methodology has the potential for both methodological and scientific applications.

The paper is structured as follows. Section 2 describes basic assumptions on the error correlation. We then introduce the new class of kernel functions and demonstrate the procedure for bandwidth selection using local linear regression. The estimation of the error covariance function is introduced and studied in Section 3. In Section 4, we evaluate the performance of our method through simulation studies. Section 5 is dedicated to a real-data application. Potential directions for future research are discussed in Section 6. Most of the key theoretical results are included in the Appendix and all proofs, additional simulation results and applications are given in the Supplementary file.

2 | BANDWIDTH SELECTION

2.1 | Method and theoretical properties

First, we introduce some notations for the rest of the paper. We will use $\|\cdot\|$ to denote the standard Euclidean norm and use notation $a_n \asymp b_n$ to indicate that both a_n/b_n and b_n/a_n are bounded (in probability) as $n \rightarrow \infty$. Denote the unit vector with 1 in the first position by $\mathbf{e}_1 = (1, 0, \dots, 0)^T$. Let $\mathbf{Y} = (Y_1, \dots, Y_n)^T$ be the vector of all observations and $\mathbf{X}_{\mathbf{x}}$ be the design matrix at point $\mathbf{x} \in \mathcal{X}$ with i -th row to be $(1, (\mathbf{X}_i - \mathbf{x})^T)$.

Considering the nonparametric regression model (1), it is common to assume that observations located close to each other are more related than those further apart. For instance, Brabanter et al⁹ assumes a short-range correlation with statistical dependence that decays rapidly to 0 as the distance between points increases. In this article, we allow for a slower decay rate, which goes beyond the assumption of short-range dependence, and propose the following assumptions.

A1: For some positive number $0 < \alpha \leq 1$, there exist positive constants C_{\max} and C_{ρ} such that,

$$n^{\alpha} \int |\rho_n(\|\mathbf{u}\|)| d\mathbf{u} < C_{\max} \text{ and } \lim_{n \rightarrow \infty} n^{\alpha} \int \rho_n(\|\mathbf{u}\|) d\mathbf{u} = C_{\rho}.$$

A2: There exists sequence $\tau_n = O(n^{-\frac{\alpha}{D+4}})$, such that

$$\lim_{n \rightarrow \infty} n^{\alpha} \int_{\|\mathbf{u}\| \geq \tau_n} |\rho_n(\|\mathbf{u}\|)| d\mathbf{u} = 0.$$

A3: For all i, j, k, l ,

$$\begin{aligned} \text{Cov}(\varepsilon_i \varepsilon_j, \varepsilon_k \varepsilon_l | \mathbf{X}_i, \mathbf{X}_j, \mathbf{X}_k, \mathbf{X}_l) &= \text{Cov}(\varepsilon_i, \varepsilon_k | \mathbf{X}_i, \mathbf{X}_k) \text{Cov}(\varepsilon_j, \varepsilon_l | \mathbf{X}_j, \mathbf{X}_l) \\ &\quad + \text{Cov}(\varepsilon_i, \varepsilon_l | \mathbf{X}_i, \mathbf{X}_l) \text{Cov}(\varepsilon_j, \varepsilon_k | \mathbf{X}_j, \mathbf{X}_k) \end{aligned}$$

Assumption A3 is satisfied, for example, when the errors follow a normal distribution. Assumption A1 indicates that the correlation function $\rho_n(\cdot)$ depends on n and that $\int \rho_n(\|\mathbf{u}\|) d\mathbf{u}$ should vanish at a rate not slower than $O(n^{-\alpha})$. Assumption A2 shows that $\int |\rho_n(\|\mathbf{u}\|)| d\mathbf{u}$ is dominated when $\|\mathbf{u}\| \leq \tau_n$. Note that when $\alpha = 1$ and τ_n is of the order $n^{-\frac{1}{D}}$, $\rho_n(\cdot)$ corresponds to the short-range correlation function in Brabanter et al⁹. However, assumptions A1 and A2 are much looser, which allows a slower decay rate of $\int \rho_n(\|\mathbf{u}\|) d\mathbf{u}$ and $\rho_n(\|\mathbf{u}\|)$ respectively. For instance, the correlation function

$$\rho_n(\|\mathbf{u}\|) = e^{-cn^{\frac{\alpha}{D}} \|\mathbf{u}\|}, \quad c > 0,$$

satisfies the assumptions A1 and A2. The decay rate is slower than that of the (short-range) correlation function, $\rho_n(\|\mathbf{u}\|) = e^{-cn^{\frac{1}{D}} \|\mathbf{u}\|}$, of the exponential model²¹. Moreover, assumption A2 allows τ_n to be at most of the order $n^{-\frac{\alpha}{D+4}}$. For example, we can

construct the correlation function

$$\rho_n(\|\mathbf{u}\|) = \left(e^{-n^2\|\mathbf{u}\|} + n^{-\frac{3\alpha}{D+4}}\|\mathbf{u}\| - n^{-\frac{\alpha}{D+4}}\|\mathbf{u}\|^3 \right) I\left(\|\mathbf{u}\| \leq n^{-\frac{\alpha}{D+4}}\right),$$

satisfies assumptions A1 and A2 and has a slower decay rate of $\int \rho_n(\|\mathbf{u}\|)d\mathbf{u}$.

The following bandwidth selection procedure is adapted to the situation with a slower decay rate of both $\int \rho_n(\|\mathbf{u}\|)d\mathbf{u}$ and $\rho_n(\|\mathbf{u}\|)$. The method can be widely applied to kernel-based nonparametric regression, like Nadaraya-Watson regression, Gasser-Müller regression, local linear regression, etc. Here, we use the local linear regression as an example to show the procedure. The estimator for the mean function μ in the model (1) at an arbitrary point $\mathbf{x} \in \mathcal{X}$ can be written as

$$\hat{\mu}_{h,K}(\mathbf{x}) = \mathbf{e}_1^T (\mathbf{X}_x^T \mathbf{W}_x \mathbf{X}_x)^{-1} \mathbf{X}_x^T \mathbf{W}_x \mathbf{Y}, \quad (2)$$

where \mathbf{W}_x is the $n \times n$ diagonal matrix of weights, i.e., $\text{diag}\{K(\|\mathbf{X}_i - \mathbf{x}\|/h)/h\}$, with kernel function K and bandwidth h .

A natural and computationally convenient method to estimate $\hat{\mu}_{h,K}(\mathbf{x})$, is to use the Mean Integrated Square Error (MISE) criterion, given by

$$\text{MISE}(h, K) = \mathbb{E} \left[\int f(\mathbf{x}) (\hat{\mu}_{h,K}(\mathbf{x}) - \mu(\mathbf{x}))^2 d\mathbf{x} \right],$$

where $\mathbf{X} = \{\mathbf{X}_1, \dots, \mathbf{X}_n\}$, h is the selected bandwidth and K is the kernel function used for estimating μ . To minimize the MISE, we need to select a bandwidth h and a kernel function K . It is well-known that errors are correlated, general smooth parameter selection methods such as Mallows's C_p ²² or Generalized Cross Validation (GCV) fail to obtain a reasonable bandwidth. Bimodal kernels have been proposed for bandwidth selection in univariate nonparametric regression⁷⁻⁹. They necessitate the kernel function K to satisfy $K(0) = 0$ and to be Lipschitz continuous at 0. However, when the decay rate of correlation function $\rho_n(\cdot)$ is slow, mere Lipschitz continuity at 0 may not be sufficient for effectively eliminating the correlation structure.

To accommodate the more complex correlation structures in multivariate nonparametric regression, we introduce a new class of kernel functions. Let $c_1 < c_2$ be two positive numbers. We consider the kernel function $K(\cdot)$ depending on the Euclidean norm of vector $\mathbf{u} = (u_1, \dots, u_D)^T$, that satisfies the following conditions:

C1: $K(\|\mathbf{u}\|) > 0$ for $c_1 < \|\mathbf{u}\| < c_2$ and $K(\|\mathbf{u}\|) = 0$ otherwise.

C2: $\int K(\|\mathbf{u}\|)d\mathbf{u} = 1$ and $\int u_i u_j K(\|\mathbf{u}\|)d\mathbf{u} = 0$ for any $i \neq j$.

C3: K is Lipschitz continuous on interval $[c_1, c_2]$.

We denote such kernel function by $K_z(\cdot)$ in the rest of the manuscript, where the subscript z indicates that the kernel function is zero in a neighborhood of the origin and non-zero outside this neighborhood. It is worth noting that $K_z(\cdot)$ is defined on an annular region $c_1 < \|\mathbf{u}\| < c_2$. This feature plays a crucial role in mitigating the effects of error correlation. Denote the residual sum of squares as $\text{RSS}(h, K_z) = \frac{1}{n} \sum_{i=1}^n [Y_i - \hat{\mu}_{h,K_z}(\mathbf{X}_i)]^2$. Suppose the local linear estimator at $x = \mathbf{X}_i$ can be written as $\mu(\mathbf{X}_i) = \sum_{s=1}^n c_{is} Y_s$. Then, it can be shown that

$$\text{MISE}(h, K) \approx \mathbb{E} [\text{RSS}(h, K) | \mathbf{X}] - \sigma^2 + \frac{2\sigma^2}{n} \sum_{i \neq s} c_{is} \rho_n(\|\mathbf{X}_i - \mathbf{X}_s\|) \quad (3)$$

from the supplementary. In local linear regression, the linear coefficient c_{is} is largely determined by $K\left(\frac{\|\mathbf{X}_i - \mathbf{X}_s\|}{h}\right)$. Therefore, if we use the kernel function K_z , when \mathbf{X}_i is close to \mathbf{X}_s , $\rho_n(\|\mathbf{X}_i - \mathbf{X}_s\|)$ is large, but c_{is} becomes very small because K_z is zero in the neighborhood of the origin. On the other hand, when \mathbf{X}_i is relatively far from \mathbf{X}_s , $\rho_n(\|\mathbf{X}_i - \mathbf{X}_s\|)$ is small, and c_{is} remains a positive constant. As a result, if we pick a appropriate large enough c_1 such that c_{is} is almost zero when $\rho_n(\|\mathbf{X}_i - \mathbf{X}_s\|)$ is large, the last term on the right hand side of above formula becomes small relative to $\mathbb{E} [\text{RSS}(h, K_z) | \mathbf{X}]$. Therefore, intuitively, minimizing $\text{RSS}(h, K_z)$ allows $\text{MISE}(h, K)$ to be asymptotically minimized when the kernel function is fixed as $K = K_z(\cdot)$. However, the kernel K_z is not MISE-optimal. As a well-known result, the Epanechnikov kernel (denoted as K_o) can lead to the minimization of the asymptotic MISE. Therefore, we need to find the bandwidth that asymptotically minimizes $\text{MISE}(h, K_o)$. Fortunately, the factor method²³ has been developed such that the ratio of two asymptotically MISE-optimal bandwidths for two different kernel functions is a constant, which depends only on the kernel functions. Thus, we can employ the factor method to obtain the asymptotically MISE-optimal bandwidth for the kernel function K_o .

Based on the motivation above, we propose the following procedure to select h for estimating μ .

Step 1: Pick a kernel K_z with a appropriate large enough c_1 value, select a bandwidth, denoted as $\hat{h}(K_z)$, that minimizes the residual sum of squares:

$$\text{RSS}(h, K_z) = \frac{1}{n} \sum_{i=1}^n (Y_i - \hat{\mu}_{h, K_z}(\mathbf{X}_i))^2, \quad (4)$$

Step 2: Calculate

$$\hat{h}(K_o) = \hat{h}(K_z) \left(\frac{\mu(K_o^2) \mu_2(K_z)^2}{\mu_2(K_o)^2 \mu(K_z^2)} \right)^{\frac{1}{D+4}}, \quad (5)$$

where $\mu_2(K) = \int u_1^2 K(\|\mathbf{u}\|) d\mathbf{u}$ and $\mu(K^2) = \int K^2(\|\mathbf{u}\|) d\mathbf{u}$.

Step 3: Substitute $K = K_o$ and $h = \hat{h}(K_o)$ into (2) to obtain the estimate of local linear regression function.

Note that the above procedure does not require estimating correlation function $\rho_n(\cdot)$. This results in a flexible method for estimating the regression function in the presence of correlated errors. In step 1, we apply the kernel function K_z to eliminate correlation, the selected $\hat{h}(K_z)$ can asymptotically minimize MISE when the kernel function is K_z . However, the kernel K_z is not MISE-optimal with fixed bandwidth, in step 2, we employ the factor method to determine the bandwidth suitable for the MISE-optimal kernel function K_o .

The following theorem presents the asymptotic results regarding the selected bandwidth $\hat{h}(K_o)$ and the MISE achieved.

Theorem 1. Suppose assumptions A1 to A3 hold. Minimizing (4) with the candidate set of bandwidth $h \in \mathcal{H}_n = (a_1 n^{-\frac{\alpha}{D+4}}, a_2 n^{-\frac{\alpha}{D+4}})$, where a_1 and a_2 are some positive constant, we obtain $\hat{h}(K_o)$ via (5). Let h^* be the bandwidth that minimizes MISE with the kernel function $K_o(\cdot)$. Then,

$$\frac{\text{MISE}(\hat{h}(K_o), K_o)}{\text{MISE}(h^*, K_o)} = 1 + o_p(1), \quad \frac{|\hat{h}(K_o) - h^*|}{h^*} = o_p(1)$$

and

$$\text{MISE}(\hat{h}(K_o), K_o) = C_1 n^{-\frac{4\alpha}{D+4}} \left[\mu(K_o^2)^2 \mu_2(K_o)^D \right]^{\frac{2}{D+4}} + o_p \left(n^{-\frac{4\alpha}{D+4}} \right),$$

where

$$C_1 = \begin{cases} 2 \left(\frac{\Delta_f}{2} \right)^{\frac{D}{D+4}} \left(\sigma^2 C_\rho \right)^{\frac{4}{D+4}}, & 0 < \alpha < 1, \\ 2 \left(\frac{\Delta_f}{2} \right)^{\frac{D}{D+4}} \left(\sigma^2 (C_\rho + m(\mathcal{X})) \right)^{\frac{4}{D+4}}, & \alpha = 1, \end{cases}$$

with $m(\mathcal{X}) = \int_{\mathbf{x} \in \mathcal{X}} 1 d\mathbf{x}$ and $\Delta_f = \int f(\mathbf{x}) \left(\sum_{d=1}^D \frac{\partial^2 \mu(\mathbf{x})}{\partial x_d^2} \right) d\mathbf{x}$.

Theorem 1 states that through the aforementioned bandwidth selection procedure, we can achieve an optimal estimation of $\mu(\cdot)$ in terms of minimizing the asymptotic MISE. Building upon the proof of the above theorem, the following result emerges.

Corollary 1. Suppose that conditions in Theorem 1 hold. Let $\hat{\mu}_{h, K_o}(\cdot)$ be the estimator (2) with the bandwidth $\hat{h}(K_o)$ and kernel function $K_o(\cdot)$. Then

$$\hat{\mu}_{h, K_o}(\mathbf{x}) - \mu(\mathbf{x}) = O_p(n^{-\frac{2\alpha}{D+4}}) \quad \text{for any } \mathbf{x} \in \mathcal{X}.$$

2.2 | Practical issues.

One of the practical questions is how to determine the function K_z . A simple option is to employ a fourth-degree polynomial function:

$$K_z(\|\mathbf{u}\|) = (A_z \|\mathbf{u}\|^3 + B_z \|\mathbf{u}\|^2 + C_z \|\mathbf{u}\| + D_z) I(c_1 \leq \|\mathbf{u}\| \leq c_2), \quad (6)$$

where A_z , B_z , C_z , and D_z are constants. Assuming c_1 and c_2 are fixed, to determine the coefficients A_z , B_z , C_z , and D_z involves minimizing two quantities. There are two possible choices. One of the choices is to minimize $\mu(K_z^2)$ to control the variance of MISE for the kernel K_z . The other is to minimize $[\mu(K_z^2)^2 \mu_2(K_z)^D]$, which leads to the asymptotic minimization of $\text{MISE}(h, K_z)$.

Secondly, the selection of c_1 would be important in real data analysis. From our simulation, we find that $c_2 = c_1 + 1/2$ works pretty well for various situations. In addition, we find that if c_1 is well selected, then the gap between c_1 and c_2 would be much

less concern in the simulation. Therefore, it is recommend to use $c_2 = c_1 + 1/2$ in practice. The choice of c_1 plays a important role for selecting the bandwidth h . To select bandwidth, we will propose a “elbow method” for the purpose.

From the Corollary A.2 in appendix, we showed that the bandwidth that can minimize the leading term of $\text{MISE}(h, K)$ should be proportional to $\left(\mu(K^2)/\mu_2(K)^2\right)^{\frac{1}{D+4}}$, therefore, we should have

$$\bar{C} = \left(\frac{\mu(K_z^2)}{\mu_2(K_z)^2}\right)^{\frac{1}{D+4}} / \hat{h}(K_z),$$

where \bar{C} is a constant only depends on ρ_n , μ , and f . Suppose the kernel function K_z is applied, and c_1 is large enough such that the last term of (3) is negligible, then intuitively, the bandwidth $\hat{h}(K_z)$ should approximately minimizes $\text{MISE}(h, K_z)$ as well. Therefore, at this time, the ratio of $\hat{h}(K_z)$ and $\left(\mu(K_z^2)/\mu_2(K_z)^2\right)^{\frac{1}{D+4}}$ should be approximately be a constant, or at least somehow stable.

Based on the above motivation and our large empirical studies, we propose a empirical visual method, called “elbow method”, for roughly pick c_1 values.

1. Put a candidate set with N_1 of c_1 values as $\mathcal{C}_1 = \{c_1^{(1)}, c_1^{(2)}, \dots, c_1^{(n_1)}, \dots, c_1^{(N_1)}\}$, where N_1 is a positive integer and $\mathcal{C}_2 = \mathcal{C}_1 + 0.5$.
2. For combination of $(c_1^{(n_1)}, c_2^{(n_1)})$ values, we compute the corresponding kernel function K_z as (3.6) such that the condition C1 to C3 is satisfied and $[\mu(K_z^2)^2 \mu_2(K_z)^D]$ is minimized.
3. For each K_z kernel, we use (6) to find the $\tilde{h}(K_z)$, and compute the quantity $\left(\frac{\mu(K_z^2)}{\mu_2(K_z)^2}\right)^{\frac{1}{D+4}}$ as well.
4. Compute the ratio $\left(\frac{\mu(K_z^2)}{\mu_2(K_z)^2}\right)^{\frac{1}{D+4}} / \hat{h}(K_z)$ for each K_z kernel and plot it against $\{c_1^{(1)}, c_1^{(2)}, \dots, c_1^{(n_1)}, \dots, c_1^{(N_1)}\}$.
5. Pick the **first** “elbow area” such that the ratio is roughly stabilized for the first several c_1 values as the choice to find the kernel K_z for removing the effect of ρ_n on bandwidth selection.

Figure 2 illustrates how to determine c_1 . The top two plots display the values of \bar{C} for different choices of c_1 under a spherical correlation model with $D = 2$ and $c = 2$ or $c = 4$. The bottom two plots show the corresponding MSE values for each c_1 . By comparing the top-left and bottom-left plots or the top-right and bottom-right plots, it is evident that the “elbow region” of c_1 values yields an optimal MSE.

3 | ESTIMATION OF THE COVARIANCE FUNCTION

In this section, we propose employing a nonparametric smoothing method to estimate the error covariance function $C_n(t) = \sigma^2 \rho_n(t)$ under assumptions A1 to A3. As $\rho_n(\cdot)$ varies with n , we further need the following assumption.

A4: $\rho_n(t) = \rho(n^{\frac{\alpha}{D}} t)$ for any $t \geq 0$, where $\rho(\cdot)$ is a valid correlation function unrelated to n , with bounded first and second derivatives.

Some common correlation functions satisfy assumption A4. For instance,

$$\begin{aligned} \text{Spherical:} \quad \rho_n(t) &= \left(1 - \frac{3n^{\frac{\alpha}{D}} t}{2c} + \frac{n^{\frac{3\alpha}{D}} t^3}{2c^3}\right) I(t \leq cn^{-\frac{\alpha}{D}}) \\ \text{Exponential:} \quad \rho_n(t) &= e^{-cn^{\frac{\alpha}{D}} t} \\ \text{Inverse quadratic:} \quad \rho_n(t) &= \frac{1}{1 + cn^{\frac{2\alpha}{D}} t^2}, \end{aligned}$$

where c is some positive number.

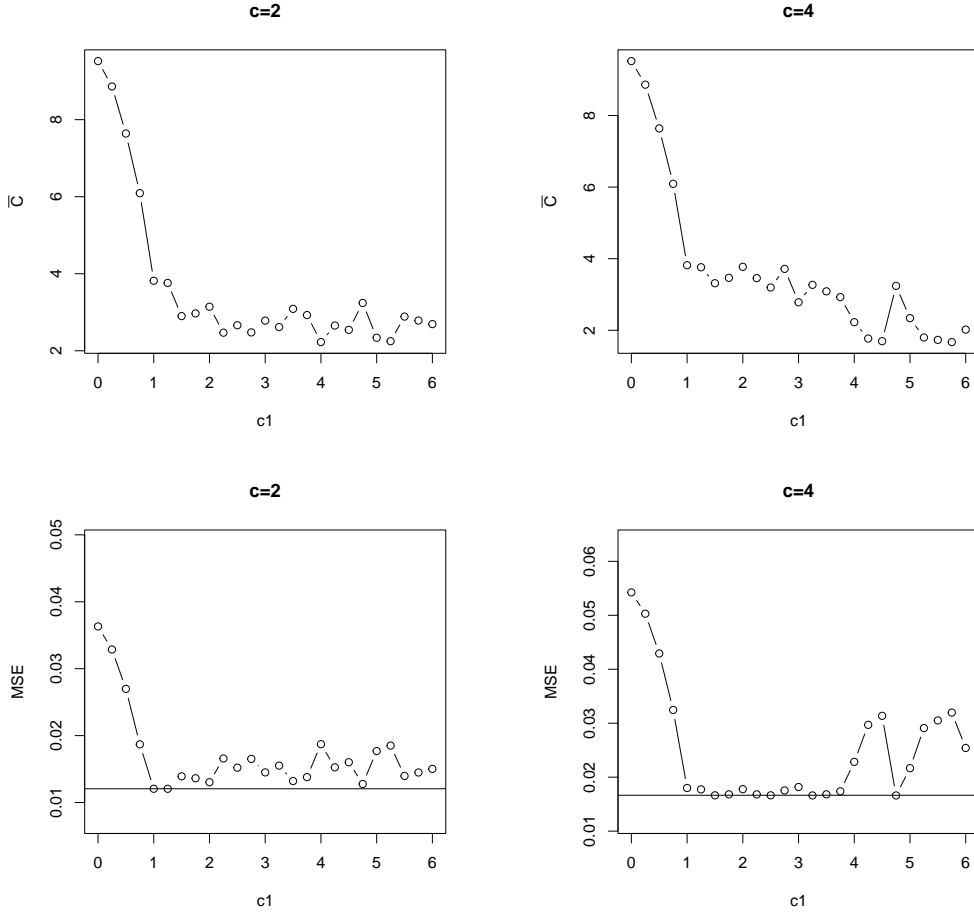


FIGURE 2 The plots comes from a typical example of our simulation trials (*seed* = 100) with spherical model and $D = 2$. In the two bottom plots, the dark solid line is the minimum MSE value we can achieve.

Suppose the assumptions A1 to A4 hold, we nonparametrically estimate covariance function $C_n(\cdot)$ use

$$\hat{C}_n(t) = \frac{\sum_{i,j=1}^n \hat{\varepsilon}_i \hat{\varepsilon}_j K_C \left(\frac{t - \|\mathbf{X}_i - \mathbf{X}_j\|}{b} \right)}{\sum_{i,j=1}^n K_C \left(\frac{t - \|\mathbf{X}_i - \mathbf{X}_j\|}{b} \right)},$$

where $\hat{\varepsilon}_i = Y_i - \hat{\mu}_{h,K_o}(\mathbf{X}_i)$, $\hat{\mu}_{h,K_o}(\mathbf{X}_i)$ is defined as (2) with kernel function K_o , b is the bandwidth to control the smoothness of $\hat{C}_n(t)$, and K_C is kernel function satisfying

$$K_C(u) > 0 \text{ for } u \in (-1, 1) \text{ and } K_C(u) = 0 \text{ otherwise,} \\ \int K_C(u) du = 1, \quad \int u K_C(u) du = 0, \quad \text{and} \quad \int u^D K_C(u) du > 0.$$

The estimator $\hat{C}_n(t)$ is closely related to the estimate of regression function in model (1) of Hall et al¹⁹. However, Hall et al¹⁹ assume one-dimensional increasing domain asymptotics which does not fit with the assumptions of model (1), whereas we assume infill asymptotics with a finite domain of \mathbf{X}_i , leading to a natural difference in theoretical investigation. To analyze the

estimator $\widehat{C}_n(t)$, we introduce the following estimator:

$$\widetilde{C}_n(t) = \frac{\sum_{i,j=1}^n \varepsilon_i \varepsilon_j K_C \left(\frac{t - \|\mathbf{X}_i - \mathbf{X}_j\|}{b} \right)}{\sum_{i,j=1}^n K_C \left(\frac{t - \|\mathbf{X}_i - \mathbf{X}_j\|}{b} \right)},$$

which assumes ε_i 's are observable.

Theorem 2. Suppose assumptions A1 to A4 hold and bandwidth b satisfies $bn^{\frac{\alpha}{D}} \rightarrow 0$ and $bn^{\alpha(1+1/D)} \rightarrow \infty$. Then, if $t \asymp n^{-\frac{\alpha}{D}}$,

$$\begin{aligned} \text{Bias} \left(\widetilde{C}_n(t) | \mathbf{X} \right) &= \mathbb{E} \left(\widetilde{C}_n(t) | \mathbf{X} \right) - C_n(t) = O_p(b^2 n^{\frac{2\alpha}{D}}), \\ \text{Var} \left(\widetilde{C}_n(t) | \mathbf{X} \right) &= O_p \left(\frac{1}{bn^{\alpha+\alpha/D}} \right). \end{aligned}$$

Theorem 2 shows that if we control b such that $b = o(n^{-\frac{\alpha}{D}})$ and $bn^{\alpha(1+1/D)} \rightarrow \infty$, then $\widetilde{C}_n(t)$ will be a consistent estimator of $C_n(t)$ for any $t \asymp n^{-\frac{\alpha}{D}}$.

We must pay careful attention to the one-dimensional case with short-range correlation. If we restrict $\alpha = 1$ and $D = 1$, then clearly, b needs to be $o(n^{-1})$. On the other hand, since X_i are random samples from a bounded f , it can be argued that $\min_{1 \leq i \leq n} |X_i - X_j| \asymp n^{-1}$. Therefore, if $b = o(n^{-1})$ and $t \asymp n^{-1}$, it can be shown that

$$\mathbb{E} \left(\sum_{i \neq j}^n I \left(|X_i - X_j| \in (t - b, t + b) \right) \middle| \mathbf{X} \right) = o_p(1).$$

It means that as $n \rightarrow \infty$, the expected number of distances $|X_i - X_j|$ inside the interval $[t - b, t + b]$ goes to 0. In that case, we are not able to obtain a valid b for the consistent estimator of $\rho_n(t)$.

Next, we state the difference between $\widehat{C}_n(t)$ and $\widetilde{C}_n(t)$ in the following results.

Theorem 3. Suppose that conditions in Theorem 2 are satisfied. We obtain $\widehat{\varepsilon}_i$ with bandwidth h and kernel function K_o . Then,

$$\widehat{C}_n(t) - \widetilde{C}_n(t) = O_p \left(\max \left\{ h^4, \frac{1}{n^\alpha h^D} \right\} \right).$$

Corollary 2. Suppose that conditions in Theorem 2 are satisfied. We obtain $\widehat{\varepsilon}_i$ with bandwidth $\widehat{h}(K_o)$ and kernel function K_o . Then, if $t \asymp n^{-\frac{\alpha}{D}}$,

$$\widehat{C}_n(t) - C_n(t) = O_p(n^{-\frac{4\alpha}{D+4}}) + O_p(b^2 n^{\frac{2\alpha}{D}}) + O_p \left(\frac{1}{\sqrt{bn^{\alpha+\alpha/D}}} \right).$$

From Corollary 2, it can be shown that choice of b matters in practice for the accuracy of $\widehat{C}(t)$. Next, we define two different variance estimators which will serve for the purposes of choosing b later on:

$$\widehat{\sigma}^2 = \frac{1}{n} \sum_{i=1}^n (Y_i - \widehat{\mu}_{h,K_o}(\mathbf{X}_i))^2, \quad \text{and} \quad (7)$$

$$\widetilde{\sigma}^2 = \widehat{C}_n(0) = \frac{\sum_{i,j=1}^n (Y_i - \widehat{\mu}_{h,K_o}(\mathbf{X}_i)) (Y_j - \widehat{\mu}_{h,K_o}(\mathbf{X}_j)) K_C \left(\frac{\|\mathbf{X}_i - \mathbf{X}_j\|}{b} \right)}{\sum_{i,j=1}^n K_C \left(\frac{\|\mathbf{X}_i - \mathbf{X}_j\|}{b} \right)}. \quad (8)$$

Theorem 4. Suppose that assumptions A1 to A4 hold. We obtain $\widehat{\mu}_{h,K_o}(\mathbf{X}_i)$ with some bandwidth h and kernel K_o , then the variance estimators (7) and (8) satisfy

$$\widehat{\sigma}^2 = \sigma^2 + O_p \left(h^4 + \frac{1}{\sqrt{n^\alpha h^D}} \right), \quad \text{and} \quad (9)$$

$$\widetilde{\sigma}^2 = \sigma^2 + O_p \left(h^4 + \frac{1}{n^\alpha h^D} \right) + O_p(bn^{\frac{\alpha}{D}}) + O_p \left(\frac{1}{b^{D/2} n^\alpha} \right), \quad (10)$$

respectively.

Theorem 4 states that $\widehat{\sigma}^2$ is a consistent estimator of σ^2 . Furthermore, it suggests that theoretically, if we specify b such that $bn^{\frac{\alpha}{D}} \rightarrow 0$ and $bn^{\alpha(1+1/D)} \rightarrow \infty$, then $|\widehat{\sigma}^2 - \sigma^2| = o_p(1)$. Consequently, $|\widetilde{\sigma}^2 - \sigma^2| = o_p(1)$. Moreover, if b satisfies these two conditions, it also fulfills the requirements of b in Corollary 2. Therefore, if we specify b to ensure $|\widetilde{\sigma}^2 - \sigma^2| = o_p(1)$, then both $\widetilde{\sigma}^2$ and $\widehat{C}_n(t)$ will be consistent estimators.

From equation (10), it is evident that a bandwidth of $h \asymp n^{-\frac{\alpha}{D+4}}$ is preferable for deriving $\widetilde{\sigma}^2$. Consequently, we employ the bandwidth $h = \widehat{h}(K_o)$ in equation (5) to calculate $\widehat{\sigma}^2$. However, according to equation (9), a bandwidth of $h \asymp n^{-\frac{\alpha}{D+8}}$ is favored for estimating $\widetilde{\sigma}^2$. Drawing from our extensive simulation study, we propose utilizing another bandwidth $h^T = \widehat{h}(K_o)n^{-\frac{1}{D+8}} / n^{-\frac{1}{D+4}}$. Clearly, when $\alpha = 1$, $h^T \asymp n^{-\frac{1}{D+8}}$.

Additionally, according to Theorem 2, if b is excessively small, the bias of $\widehat{C}_n(t)$ will be minimal, yet this results in a high variation in the fitted covariance function. Conversely, with increasing in b , the variance of $\widehat{C}_n(t)$ decreases, but its bias begins to increase.

Given the aforementioned analysis, we introduce a practical approach for determining b , which we refer to as the ‘‘Variance-calibration’’ procedure:

- Step 1.** Specify a candidate set $\mathcal{B} = \{b_1, b_2, \dots, b_M\}$ with $b_1 < b_2 < \dots < b_M$, ensuring that the initial segment of \mathcal{B} is sufficiently small to observe distinct undersmoothing in the fitted covariance function.
- Step 2.** Estimate $\widetilde{\sigma}^2$ using equation (7) with bandwidth $h^T = \widehat{h}(K_o)n^{-\frac{1}{D+8}} / n^{-\frac{1}{D+4}}$.
- Step 3.** Estimate $\widehat{\sigma}^2$ using equation (8) with bandwidth $\widehat{h}(K_o)$.
- Step 4.** Fit $C_n(t)$ using b_1, b_2, \dots, b_M , and choose the largest bandwidth such that $|\widehat{\sigma}^2 - \widetilde{\sigma}^2|$ is less than a small positive value δ_n .

The fundamental idea is to find the largest b value that still allows for a consistent estimator $\widetilde{\sigma}^2$ for σ^2 and a small bias of $\widehat{C}_n(t)$ when t is close to 0. With this b , we can achieve a smooth fit of $C_n(t)$ in the neighborhood of 0 and the consistency of σ^2 and $\widehat{C}_n(t)$. In real data applications, we also recommend combining the above procedure with visualization. That is, we plot the fitted $\widehat{C}_n(t)$ versus t with different bandwidth b , which can assist us to observe the clear pattern of underestimation and overestimation with varied b 's and identify the b that almost aligns $\widehat{\sigma}^2$ and $\widetilde{\sigma}^2$ and gives the smoothest curve.

Figure 3 illustrates this procedure. The top-left panel shows the significant variance in $\widehat{C}_n(t)$ when b is too small. The bottom-right panel indicates that when b is too large, $\widehat{C}_n(t)$ overfit with significant bias in the neighborhood of 0. In contrast, the top-right panel shows that $b = 0.015$ is just right for fitting $C_n(t)$ in the neighborhood of 0, where we have calibrated the $\widehat{\sigma}^2$ with σ^2 . The ‘‘Variance-calibration’’ method essentially involves gradually increasing b until $\widehat{\sigma}^2$ aligns with the $\widetilde{\sigma}^2$. Our simulations indicate that as long as $\widetilde{\sigma}^2$ is accurately estimated, $C_n(t)$ can be well estimated in the vicinity of 0.

Theoretically, we have demonstrated that $C_n(t)$ will be consistent for $t \asymp n^{-\frac{\alpha}{D}}$ provided that b is chosen appropriately. When $n^{-\frac{\alpha}{D}} = o(t)$, $C_n(t)$ tends to zero as $n \rightarrow \infty$. Consequently, in practical applications, we recommend setting $\widehat{C}_n(t)$ to zero when t exceeds a certain threshold. For instance, as depicted in Figure 3, our interest in covariance estimation would typically be limited to when $t \leq 0.1$, the region where $C_n(t)$ is very close to zero generally does not significantly impact data analysis.

After choosing b , we take

$$\widehat{\rho}_n(t) = \frac{\widehat{C}_n(t)}{\widehat{C}_n(0)} \quad \text{or} \quad \widehat{\rho}_n(t) = \frac{\widehat{C}_n(t)}{\widehat{\sigma}^2} \quad (11)$$

as the estimation of $\rho_n(t)$. Asymptotically, the difference of $\widehat{C}_n(0)$ and $\widehat{\sigma}^2$ is negligible. Theorem 4 also shows that as α decreases from 1, the estimation of σ^2 will be less efficient. The ‘‘Variance-calibration’’ uses this as a reference, which leads to a less efficient estimator of C_n if σ^2 is not well-estimated. Nevertheless, the estimator $\widehat{\rho}_n$ will be less affected since the division cancel out the $\widehat{\sigma}^2$. This may be helpful for analysis of the correlation among different samples.

One of the practical issues is that there is $O(n^2)$ of $C_n(\|\mathbf{X}_i - \mathbf{X}_j\|)$ need to be estimated, with moderately large n , this could be computational very time-consuming. Therefore, we suggest to estimate $C_n(t)$ at discrete points t_0, t_1, \dots, t_{n^*} , where $n^* \ll n^2$ with $t_0 = 0$. Next, we interpolate the estimates $\widehat{C}_n(t_1), \dots, \widehat{C}_n(t_{n^*})$ to get $\widehat{C}_n(t)$.

Although theoretically, the bandwidth b less than t is desired for the consistency of $\widehat{\rho}_n(t)$, in practice, estimation of $\rho_n(t)$ close to 0 is important since $\rho_n(t)$ is generally large when data points are close. We suggest using the boundary kernel function when the estimation location t is smaller than b in real data applications. From our simulation study, it is recommended to use the

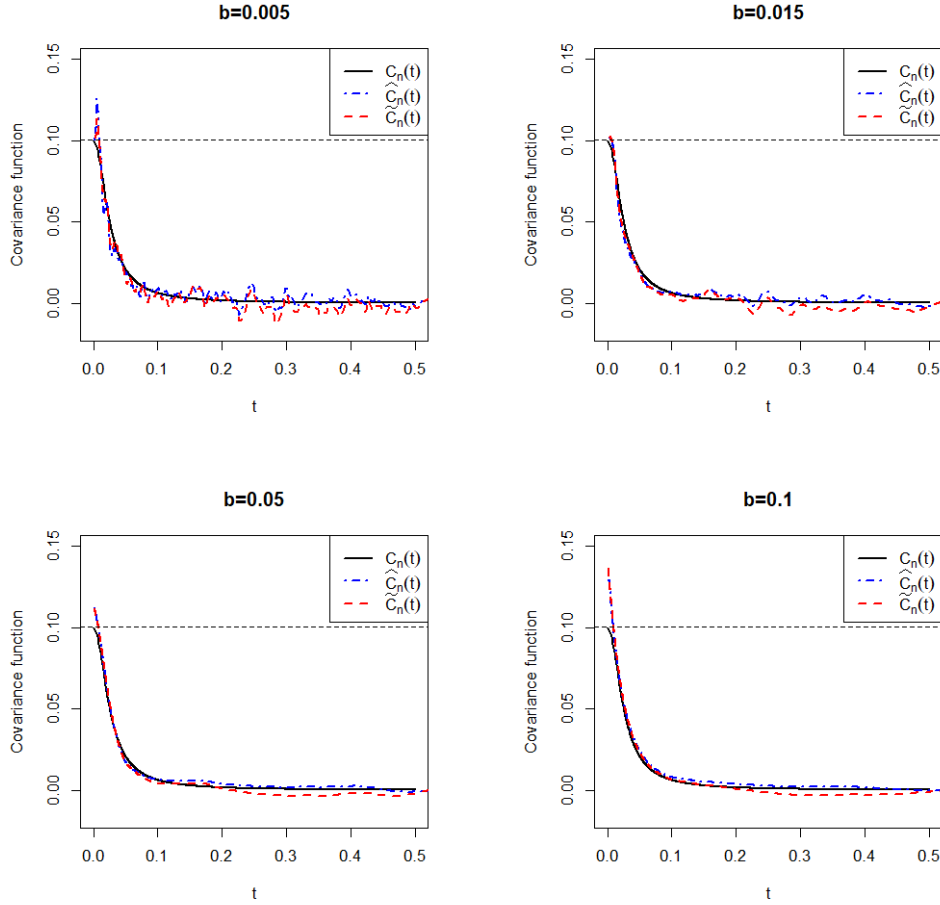


FIGURE 3 Results with a two-dimensional spherical covariance with $\sigma^2 = 0.1$. The solid black line, blue dot-dashed line, and red dashed line represent the true covariance function $C_n(t)$, the estimated covariance functions $\hat{C}_n(t)$ and $\tilde{C}_n(t)$ respectively. The black dashed horizontal line stands for σ^2 .

boundary kernel function proposed in Müller and Wang²⁴ as

$$K(t) = \frac{12(t+1)}{(1+q)^4} \left(t(1-2q) + \frac{(3q^2-2q+1)}{2} \right) I(|t| \leq 1), \quad (12)$$

where $q = \frac{t}{b}$ if $t < b$ and $q = 1$ if $t \geq b$. If $q = 1$, $K(t)$ is the Epaninikov kernel function.

4 | NUMERICAL STUDY

In this section, we conduct simulations to evaluate the proposed method outlined in Sections 2 and 3. We examine three distinct correlation functions as detailed in Section 3 within our simulation study. We generate data from model (1) considering either $D = 2$ or $D = 3$. The corresponding regression functions are $\mu(\mathbf{X}_i) = 2X_{i1}^2 + 2\cos(\pi X_{i2})$ for $i \in \{1, \dots, 500\}$ and $\mu(\mathbf{X}_i) = X_{i1} + \sin(\pi X_{i2}) + 2X_{i3}^2$ for $i \in \{1, \dots, 600\}$, where \mathbf{X}_i are random vectors with each component independently generated from Uniform(0, 1). In each simulation scenario, we set $\sigma^2 = 0.1$ and $\alpha = 1$. The parameter c is varied to control the intensity of the error correlation. Several correlation functions with different values of c when $D = 2$ are illustrated in Figure 4. Due to space limitations, we only present simulation results for the case of $D = 2$. Simulation results for $D = 3$ will be included in the Supplementary file.

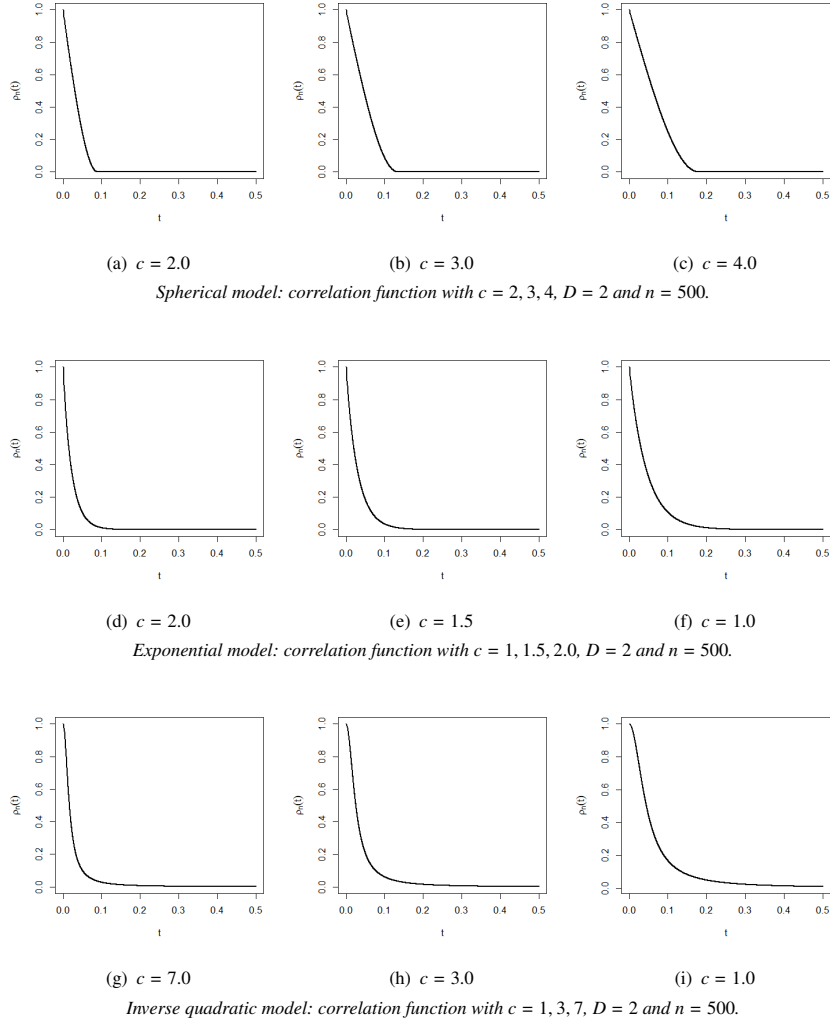


FIGURE 4 Examples of three different correlation functions with different c values.

4.1 | Estimation of regression function

We use local linear fitting to obtain estimates of the regression function as given by (2). The performance of the regression estimator is evaluated using the following metric:

$$\text{MSE}_{\text{prac}}(h) = \frac{1}{n} \sum_{i=1}^n (\hat{\mu}_{h,K}(\mathbf{X}_i) - \mu(\mathbf{X}_i))^2,$$

where h represents the bandwidth used for regression estimation and K is the kernel function used to derive the local linear estimator. In our simulation, we compare three different methods for bandwidth selection: (a) The Epsilon-class method proposed in Brabanter et al⁸ with $\varepsilon = 0.1$ (denoted as “Eps”). (b) The Exponential kernel function proposed in the discussion of Brabanter et al⁹ with the factor method (denoted as “Exp”). (c) Our procedure with proposed kernel function K_z with $(c_1, c_2) = (1.0, 1.5)$, $(c_1, c_2) = (2.0, 2.5)$, or $(c_1, c_2) = (3.0, 3.5)$ (denoted as “ZA(c_1, c_2)”). For each pair of c_1 and c_2 , we minimize $[\mu(K_z^2)\mu_2(K_z)]$ to obtain the coefficients of K_z . For “Exp” and “ZA(c_1, c_2)”, which require an optimal K_o for the factor procedure, we use the product Epanechnikov kernel function as $K_o(\mathbf{u}) = \prod_{d=1}^D K(u_d)$, with $K(u) = \frac{3}{4}(1 - u^2)I(|u| \leq 1)$, and the same bandwidth for each direction.

We present the mean and standard deviation of MSE_{prac} with the bandwidth selected from the above methods. Additionally, the mean and standard deviation of the minimum MSE_{prac} that can be achieved by the product Epanechnikov kernel is computed as the reference line of each method (denoted as “minEpan”). For each simulation scenario, we repeat 100 trials. Table 1 presents the mean and standard deviation of MSE_{prac} for different values of c . “SP”, “EXP” and “INVQ” stand for Spherical model, Exponential model and Inverse quadratic model respectively.

TABLE 1 Mean and standard deviation (in parentheses) of MSE_{prac} values ($\times 10^{-2}$) in each simulation scenario from 100 trials. The regression function is $\mu(\mathbf{X}) = 2X_1^2 + 2\cos(\pi X_2)$, sample size $n = 500$, and $\sigma^2 = 0.1$.

Model	method	minEpan	Epsilon	Exp	ZA(1,1.5)	ZA(2,2.5)	ZA(3,3.5)
SP	$c = 1.0$	0.73(0.22)	1.18(0.46)	0.91(0.37)	0.80(0.24)	0.92(0.29)	1.18(0.49)
	$c = 2.0$	1.15(0.32)	2.99(0.75)	2.54(0.40)	1.31(0.39)	1.28(0.36)	1.38(0.46)
	$c = 3.0$	1.68(0.52)	4.15(0.91)	3.75(0.66)	2.09(0.64)	1.84(0.60)	1.89(0.66)
	$c = 4.0$	2.40(0.84)	5.14(1.16)	4.79(0.92)	3.11(0.96)	2.61(0.87)	2.62(0.90)
EXP	$c = 2.5$	0.85(0.22)	1.42(0.46)	1.34(0.41)	0.92(0.24)	1.04(0.31)	1.25(0.48)
	$c = 2.0$	0.96(0.29)	1.93(0.60)	1.75(0.44)	1.03(0.30)	1.12(0.36)	1.32(0.48)
	$c = 1.5$	1.16(0.40)	2.59(0.75)	2.31(0.50)	1.28(0.44)	1.31(0.51)	1.45(0.55)
	$c = 1.0$	1.56(0.46)	3.54(0.84)	3.22(0.56)	1.84(0.48)	1.67(0.48)	1.82(0.57)
INVQ	$c = 10.0$	0.93(0.28)	1.62(0.55)	1.49(0.49)	1.02(0.31)	1.07(0.35)	1.24(0.45)
	$c = 7.0$	0.99(0.31)	1.95(0.59)	1.70(0.50)	1.06(0.33)	1.10(0.38)	1.30(0.48)
	$c = 3.0$	1.40(0.47)	3.03(0.77)	2.70(0.49)	1.59(0.48)	1.53(0.50)	1.65(0.56)
	$c = 1.0$	2.06(0.74)	4.51(0.99)	4.11(0.83)	2.53(0.84)	2.27(0.78)	2.29(0.83)

From Table 1, it is evident that the minimum MSE_{prac} increases as $\rho_n(t)$ increases. Bimodal kernel functions that are Lipschitz continuous at 0 are less efficient at removing the effects of error correlation compared to the kernel function K_z , such as the Epsilon-class function and the Exponential function. Comparing the three different sets of (c_1, c_2) pairs, it can be seen that when the correlation function is centered around 0, “ZA(1, 1.5)” performs the best among all five methods. This is plausible because when c_1 is smaller, the quantity $[\mu(K_z^2)\mu_2(K_z)]$ will be smaller, resulting in a smaller MSE value. On the other hand, when the error correlation is strong, a small c_1 may not be sufficient to mitigate such correlation effect, leading to a larger MSE. Therefore, we observe better performance of “ZA(2, 2.5)” or “ZA(3, 3.5)” when the correlation function is more distant from 0, such as the Spherical model with $c = 4.0$ or the Inverse quadratic model with $c = 1.0$.

4.2 | Estimation of covariance function

Next, we investigate the performance of $\widehat{\sigma^2}$ and the correlation function estimator $\widehat{\rho}_n(t)$. We compare the three different methods mentioned in section 4.1. Additionally, we use the estimator computed assuming the errors are known as the reference line for comparison. This includes the variance estimator $\widehat{\sigma^2} = \frac{1}{n} \sum_{i=1}^n \varepsilon_i^2$ and covariance estimator $\widetilde{C}_n(t)$. (denoted as “Raw”).

First, we study the simulation results of $\widehat{\sigma^2}$, which is computed as in equation (7). The $\widehat{\varepsilon}_i$ are obtained via $\widehat{\varepsilon}_i = Y_i - \widehat{\mu}_{h^T, K_o}(\mathbf{X}_i)$ with $h^T = \widehat{h}n^{-\frac{1}{D+8}}/n^{-\frac{1}{D+4}}$, where \widehat{h} is the bandwidth chosen from the three different methods in section 4.1. We use

$$MSE_{\widehat{\sigma^2}} = \frac{1}{N_T} \sum_{T=1}^{N_T} \left(\widehat{\sigma^2}^{(T)} - \sigma^2 \right)^2$$

to measure the performance of $\widehat{\sigma^2}$, where N_T is the number of trials in the simulation and $\widehat{\sigma^2}^{(T)}$ is the variance estimator of T -th simulation trial.

From Tables 2, it is observed that when the correlation function is relatively large, using proposed kernel K_z will lead to a smaller $MSE_{\widehat{\sigma^2}}$ compared to the Epsilon-class kernel and Exponential kernel. Additionally, as the correlation function becomes stronger, using K_z that is farther away from 0 can provide a better estimation of σ^2 . However, we can see that if the correlation function is small, the Epsilon-class kernel may provide a better estimation of σ^2 . This suggests that if the correlation function is very weak, using the Epsilon-class kernel may lead to better bandwidth selection for variance estimation. Nonetheless, the purpose of this article is to pursue better performance when the correlation function is not predominantly centered around 0.

TABLE 2 $MSE_{\hat{\sigma}_2^2} (\times 10^{-5})$ in each simulation scenario from 100 trials. The regression function is $\mu(\mathbf{X}) = 2X_1^2 + 2\cos(\pi X_2)$, sample size $n = 500$, and $\sigma^2 = 0.1$.

Model	method	Raw	Epsilon	Exp	ZA(1,1.5)	ZA(2,2.5)	ZA(3,3.5)
SP	$c = 1.0$	4.60	9.89	8.69	10.23	20.59	38.79
	$c = 2.0$	6.49	18.17	56.55	10.16	20.18	29.31
	$c = 3.0$	10.49	97.07	141.83	24.66	18.70	23.36
	$c = 4.0$	16.44	224.37	260.00	74.60	25.27	23.65
EXP	$c = 2.5$	4.52	6.56	12.86	8.34	18.91	34.88
	$c = 2.0$	4.82	4.79	23.70	8.86	17.80	34.81
	$c = 1.5$	5.53	10.90	46.87	10.53	15.66	33.48
	$c = 1.0$	7.79	48.20	103.36	16.54	10.78	27.65
INVQ	$c = 10.0$	4.68	5.21	15.15	8.53	15.15	29.09
	$c = 7.0$	4.94	5.58	23.41	7.17	14.01	34.71
	$c = 3.0$	6.28	20.95	64.69	11.51	11.14	22.65
	$c = 1.0$	11.27	117.53	173.16	36.83	15.74	23.40

Second, we investigate the performance of the correlation estimator $\hat{\rho}_n(\cdot)$. We employ the ‘‘Variance-calibration’’ procedure described in section 3 to select the bandwidth b , aiming to find the largest b such that $|\hat{C}_n(0) - \hat{\sigma}^2| \leq \delta_n$. In our simulation, we set $\delta_n = 2 \times 10^{-4}$. After determining b , we estimate $\hat{\rho}_n(t)$ via (11) with the boundary kernel in (12). To evaluate the performance of $\hat{\rho}_n(t)$, we use the following quantity:

$$SSE_{\text{cor}} = \sum_{i=1}^n \sum_{j=i+1}^n \left\{ \hat{\rho}_n(\|\mathbf{X}_i - \mathbf{X}_j\|) - \rho_n(\|\mathbf{X}_i - \mathbf{X}_j\|) \right\}^2 I\left(\rho_n(\|\mathbf{X}_i - \mathbf{X}_j\|) \leq \zeta\right),$$

and ζ is a positive threshold used to truncate the correlation estimation when $\rho_n(\|\mathbf{X}_i - \mathbf{X}_j\|)$ is smaller than ζ . In our simulation, the threshold ζ is set as 0.02. Basically, SSE_{cor} measures the performance of correlation estimator when the real correlation is greater than ζ .

Table 3 presents the simulation results of SSE_{cor} for 2-D models respectively. When the correlation is small, such as in the first line of each correlation model in Table 3, we observe that the SSE_{cor} values from the ‘‘Raw’’ method, where ε is treated as known, are relatively large compared to others. This is not surprising since $\hat{\varepsilon}$ will be close to ε when the correlation is small, and the estimation error of covariance will mostly come from the difference between $\hat{\rho}_n(t)$ and $\rho_n(t)$.

On the other hand, when the correlation is large, the SSE_{cor} values from the ‘‘Raw’’ method are much smaller than others. In this case, the estimation error will be dominated by the error from $\hat{\rho}_n(t)$. It is observed that using the proposed kernel K_z performs better than the Epsilon-class kernel and the Exponential kernel most of the time. From section 2, we know that if the correlation is large, kernel function K_z with a larger c_1 value leads to a better choice of bandwidth, hence $\hat{\varepsilon}_i$ provides a better estimation of ε_i . Thus, we can see that as the correlation function increases, a kernel function that is farther away from 0 will lead to a better estimation of covariance.

TABLE 3 Mean and standard deviation (in parentheses) of SSE_{cor} values in each simulation scenario from 100 trials. The regression function is $\mu(\mathbf{X}) = 2X_1^2 + 2\cos(\pi X_2)$, sample size $n = 500$, $\sigma^2 = 0.1$. ‘‘SP’’, ‘‘EXP’’ and ‘‘INVQ’’ stand for Spherical model, Exponential model and Inverse quadratic model respectively.

Model	method	Raw	Epsilon	Exp	ZA(1,1.5)	ZA(2,2.5)	ZA(3,3.5)
SP	$c = 1.0$	4.68(3.02)	25.36(20.17)	3.19(2.19)	5.96(4.24)	10.27(6.77)	16.01(10.57)
	$c = 2.0$	20.12(21.87)	256.02(68.45)	183.65(21.81)	70.90(37.93)	41.70(25.26)	31.21(18.11)
	$c = 3.0$	38.98(52.57)	700.10(58.56)	654.62(37.61)	386.78(130.57)	258.42(113.41)	181.93(100.54)
	$c = 4.0$	95.76(82.52)	1489.61(101.99)	1410.76(83.30)	1052.23(201.80)	710.70(224.53)	494.16(205.60)
EXP	$c = 2.5$	13.06(6.26)	82.23(44.72)	19.30(14.22)	16.54(10.83)	20.42(12.21)	29.72(17.99)
	$c = 2.0$	13.55(9.42)	146.80(65.72)	40.43(18.09)	19.77(16.82)	13.59(12.35)	19.92(27.84)
	$c = 1.5$	17.72(18.64)	249.80(87.42)	121.38(21.71)	60.93(38.52)	32.48(26.65)	21.23(28.10)
	$c = 1.0$	53.18(44.40)	545.45(109.27)	429.50(31.27)	282.89(85.04)	172.75(88.18)	100.63(69.01)
INVQ	$c = 10.0$	20.76(18.84)	127.91(49.61)	40.12(18.42)	30.03(19.40)	20.62(13.00)	32.13(26.81)
	$c = 7.0$	21.18(17.03)	181.10(70.73)	64.73(22.97)	36.88(26.18)	21.34(20.42)	26.99(29.41)
	$c = 3.0$	44.75(47.74)	391.20(91.25)	230.44(36.12)	151.02(62.29)	90.91(52.40)	54.99(39.31)
	$c = 1.0$	289.11(177.85)	1081.67(112.79)	977.74(51.45)	723.42(136.64)	554.78(148.01)	409.89(179.55)

5 | APPLICATION TO CARDIOVASCULAR DISEASE MORTALITY RATES DATA SET

We return to the dataset on Cardiovascular Disease Mortality Rates. Figure 1(a) shows the mortality rates (deaths per 1000 population) for cardiovascular disease from 1064 counties in the Southeastern United States in the year 2014. In Figure 1, there is no clear monotonic trend. Instead, several areas show high mortality rates, such as eastern Kentucky, inner Georgia, and the region where Mississippi, Arkansas, and Louisiana intersect. This suggests that a parametric regression might not be suitable. Therefore, we used the bandwidth selection procedure from Section 2 to fit the regression surface of the mortality rate. We then utilized the residuals and the methods detailed in Section 3 to estimate the error covariance function.

For comparison purposes, we applied the three methods described in Section 2.2 to 4.1 for bandwidth selection. In addition, we employed the C_p criterion with the product Epanichikov kernel (referred to as “Epan”), which does not consider the error correlation at all. The “elbow method” was applied to seek for an appropriate c_1 . Figure 5 present the visualization of c_1 against \bar{C} , when the candidate set of c_1 is $\{0, 0.25, \dots, 5.75, 6.00\}$ and $c_2 = c_1 + 0.5$. Based on Figure 5, we pick $c_1 = 1.25$ such the \bar{C} values are stable for the first time.

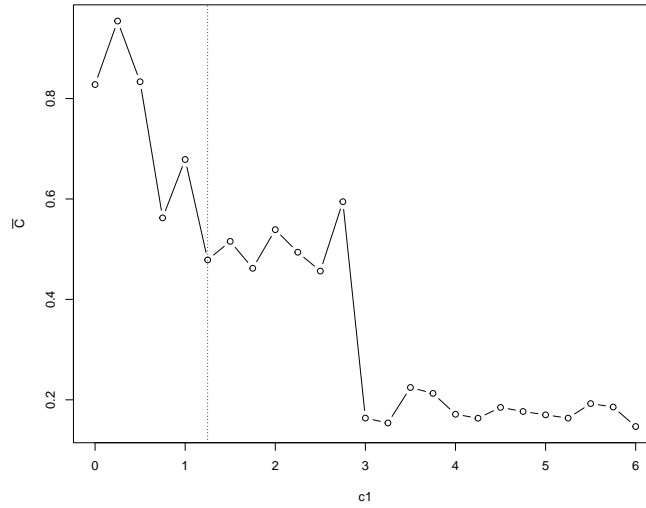


FIGURE 5 The visualization of c_1 against \bar{C} , the plot gives the choice of $c_1 = 1.25$, which corresponds to the vertical dotted line.

The panel (a) to panel (d) in Figure 6 display the fitted surface plots from four different bandwidth selections. The application of the polynomial kernel (6) in panel (d) effectively removes most of the correlation structure, resulting in a smoother surface estimation. When we employ the other three methods, the fitted surface exhibits multiple peaks, which leads to difficulty in interpretation. For better visualization, the contour plot of the panel (d) of Figure 6 is displayed in Figure 7(a). It is observed that the three areas, including eastern Kentucky, inner Georgia, and the region where Mississippi, Arkansas, and Louisiana intersect, exhibit relatively higher mortality rates compared to the surrounding regions.

Next, we aim to estimate the error correlation function to explore the relationship between the mortality rates and the geological distance of the two counties. We utilized the Haversine method to compute the actual distance between two points instead of the Euclidean distance. Figure 7(b) illustrates that the estimated correlation function decreases as the distance between two locations increases. Moreover, employing the kernel function (6) results in a more intense correlation function, which decreases slower than other estimates. It indicates that Cardiovascular Disease Mortality Rates from two counties that are more than 50km away may still related to each other. In real-world applications, the true error correlation function is unknown. However, it is evident that the correlation function estimated using bandwidth selected by the naive C_p criterion, without considering any correlation, is inappropriate. Note that the correlation functions estimated from “Eps” are very close to that from “Epan”. This suggests that the epsilon-class may not behave well for the correlation estimation in this application.

Remark: In addition to the Cardiovascular Disease Mortality Rates data, we extracted Life Expectancy and Colon & Rectum cancer mortality rates for all counties in the Southeastern United States from the Life Expectancy Data and Cancer Mortality Rates data respectively. We applied our methods to these two datasets as well. Please refer to the supplementary file for details

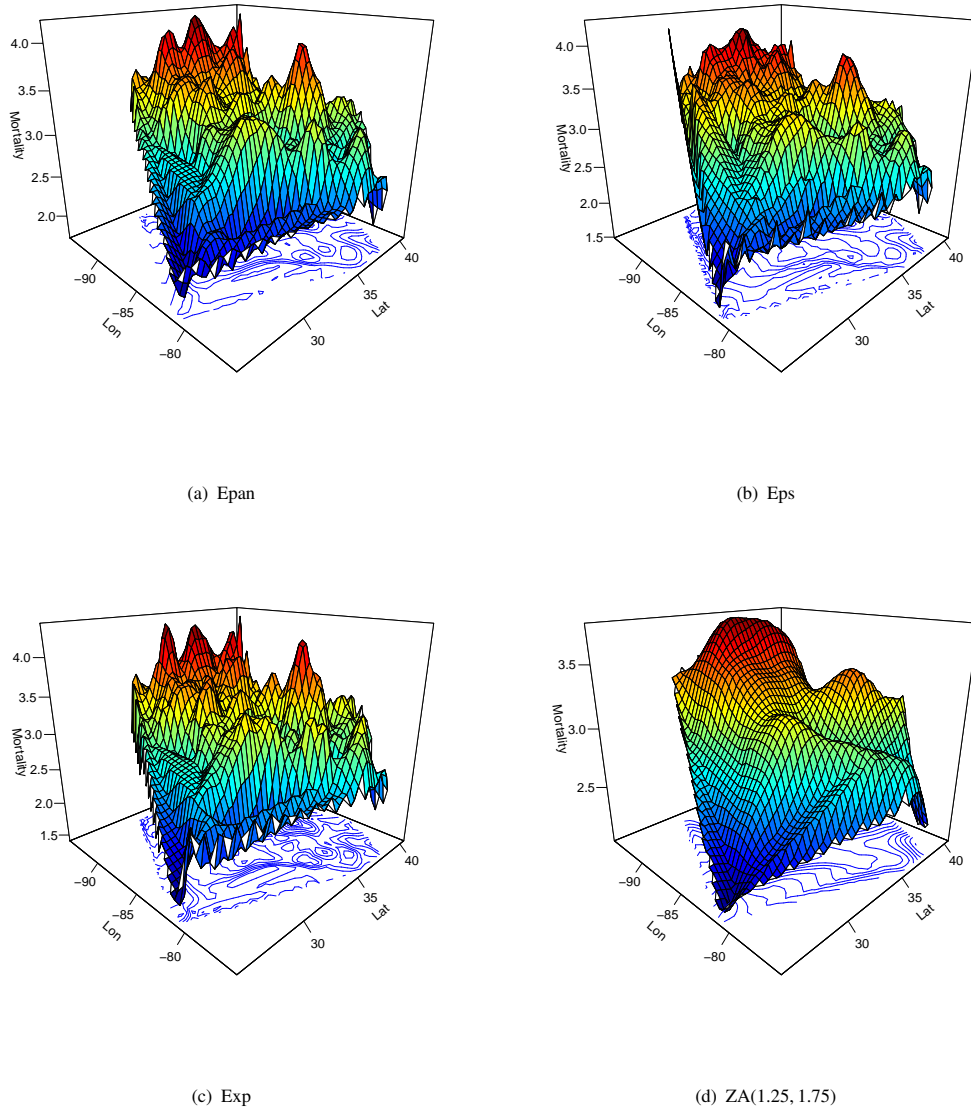


FIGURE 6 (a)*Epan*, bandwidth selected from using C_p criterion with product Epanichikov kernel; (b)*Eps*, bandwidth selected from C_p criterion with epsilon-class kernel; (c)*Exp*, bandwidth selected from exponential kernel with factor method; (d)*ZA*, bandwidth selected from Zero-apart kernel with factor method. $(c_1, c_2) = (1.0, 1.5)$.

of the additional real data applications. All three real data applications demonstrate that a bimodal kernel will not be sufficient to remove error correlation, resulting in a wiggly surface that is difficult to interpret. Moreover, the Global Health Data Exchange also contains a variety of other disease mapping data, and our methods are applicable to many of these data types.

6 | DISCUSSION

In the present article, we introduce a method for selecting the bandwidth parameter to estimate the regression function in the presence of error correlation, and we study the estimation of the error correlation function after estimating the regression function. Simulation studies showed that our proposed method performs well when the correlation function is not predominantly centered around zero. Finally, we demonstrate the application of the proposed method by analyzing Cardiovascular Disease Mortality Rates in the Southeastern United States.

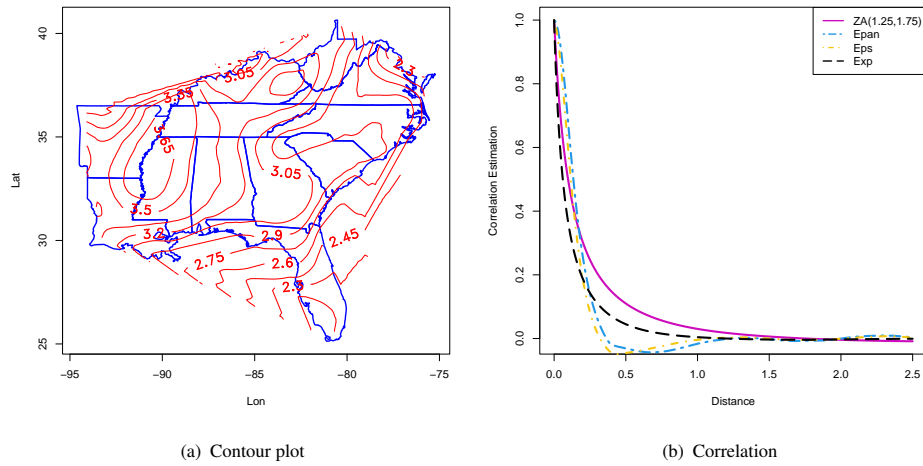


FIGURE 7 (a): contour plot of the fitted surface with the application of kernel (6). (b): relations between the estimated error correlation and distance ($\times 10^2 \text{ km}$).

We envision several directions for future research. First, the bandwidth selection method proposed for the error variance estimator, $\hat{\sigma}^2$ remains heuristic. In the future, we aim to conduct a rigorous investigation to identify a more precise approach for selecting the bandwidth for the estimation of the error covariance function. Second, it would be an interesting problem to develop a statistical test to identify where the error correlation function diminishes to 0. Third, since the Spatial-Temporal data are characterized by variations in both time and location, we plan to extend our method to accommodate spatial-temporal data models of the form $Y_i = \mu(t_i, X_i) + \varepsilon_i$ with ε_i 's are correlated, where t_i and X_i denote the observed time and location, respectively. Finally, our method still assumes homogeneous error variance, but it is worth extending it to account for heteroskedastic error variance which may fit with more real data applications.

AUTHOR CONTRIBUTIONS

Sisheng Liu worked for the Methodology development, theoretical studies, simulation, real data analysis and writing. Xiaolikong worked for the writing and theoretical studies.

ACKNOWLEDGMENTS

Sisheng Liu is supported by the National Natural Science Foundation of China (Grant 12401346) and the Natural Science Foundation of Hunan Province (Grant 2025JJ60008).

FINANCIAL DISCLOSURE

None reported.

CONFLICT OF INTEREST

The authors declare no potential conflict of interests.

REFERENCES

- [1] Jean Opsomer, Yuedong Wang, and Yuhong Yang. Nonparametric regression with correlated errors. *Statistical Science*, 16(2):134–153, 2001.
- [2] Peter Hall and Ingrid Van Keilegom. Using difference-based methods for inference in nonparametric regression with time series errors. *Journal of the Royal Statistical Society: Series B (Statistical Methodology)*, 65(2):443–456, 2003.
- [3] Mario Francisco-Fernández, Jean Opsomer, and Juan M Vilar-Fernández. Plug-in bandwidth selector for local polynomial regression estimator with correlated errors. *Nonparametric Statistics*, 16(1-2):127–151, 2004.
- [4] Mario Francisco-Fernandez and Jean D Opsomer. Smoothing parameter selection methods for nonparametric regression with spatially correlated errors. *Canadian Journal of Statistics*, 33(2):279–295, 2005.

- [5] Patrick S Carmack, William R Schucany, Jeffrey S Spence, Richard F Gunst, Qihua Lin, and Robert W Haley. Far casting cross-validation. *Journal of Computational and Graphical Statistics*, 18(4):879–893, 2009.
- [6] Patrick S Carmack, Jeffrey S Spence, and William R Schucany. Generalised correlated cross-validation. *Journal of Nonparametric Statistics*, 24(2):269–282, 2012.
- [7] Tae Yoon Kim, Byeong U Park, Myung Sang Moon, and Chiho Kim. Using bimodal kernel for inference in nonparametric regression with correlated errors. *Journal of Multivariate Analysis*, 100(7):1487–1497, 2009.
- [8] Kris De Brabanter, Jos De Brabanter, Johan AK Suykens, and Bart De Moor. Kernel regression in the presence of correlated errors. *Journal of Machine Learning Research*, 12(6), 2011.
- [9] Kris De Brabanter, Fan Cao, Irène Gijbels, and Jean Opsomer. Local polynomial regression with correlated errors in random design and unknown correlation structure. *Biometrika*, 105(3):681–690, 2018.
- [10] Sisheng Liu and Jing Yang. Kernel regression for estimating regression function and its derivatives with unknown error correlations. *Metrika*, 87(1):1–20, 2024.
- [11] Deru Kong, Shengli Zhao, and WenWu Wang. Nonparametric derivative estimation with bimodal kernels under correlated errors. *Computational Statistics*, 39(4):1847–1865, 2024.
- [12] Justin Dang and Aman Ullah. Generalized kernel regularized least squares estimator with parametric error covariance. *Empirical Economics*, 64:1–30, 2023.
- [13] Sisheng Liu and Xiaoli Kong. A generalized correlated c_p criterion for derivative estimation with dependent errors. *Computational Statistics & Data Analysis*, 171:107473, 2022.
- [14] Naomi S Altman. Kernel smoothing of data with correlated errors. *Journal of the American Statistical Association*, 85(411):749–759, 1990.
- [15] Naomi Simone Altman. Estimating error correlation in nonparametric regression. *Statistics & probability letters*, 18(3): 213–218, 1993.
- [16] Byeong U Park, Young Kyung Lee, Tae Yoon Kim, and Cheolyong Park. A simple estimator of error correlation in non-parametric regression models. *Scandinavian Journal of Statistics*, 33(3):451–462, 2006.
- [17] Kai Yang and Peihua Qiu. Nonparametric estimation of the spatio-temporal covariance structure. *Statistics in Medicine*, 38(23):4555–4565, 2019. . URL <https://onlinelibrary.wiley.com/doi/abs/10.1002/sim.8315>.
- [18] Yan Cui, Michael Levine, and Zhou Zhou. Estimation and inference of time-varying auto-covariance under complex trend: A difference-based approach. *Electronic Journal of Statistics*, 15(2):4264–4294, 2021.
- [19] Peter Hall, Nicholas I Fisher, and Branka Hoffmann. On the nonparametric estimation of covariance functions. *The Annals of Statistics*, 22(4):2115–2134, 1994.
- [20] InKyung Choi, Bo Li, and Xiao Wang. Nonparametric estimation of spatial and space-time covariance function. *Journal of Agricultural, Biological, and Environmental Statistics*, 18(4):611–630, 2013.
- [21] Noel Cressie. *Statistics for spatial data*. John Wiley & Sons, 2015.
- [22] Colin L Mallows. Some comments on c_p . *Technometrics*, 15(4):661–675, 1973.
- [23] Hans-Georg Müller, Ulrich Stadtmüller, and Thomas Schmitt. Bandwidth choice and confidence intervals for derivatives of noisy data. *Biometrika*, 74(4):743–749, 1987.
- [24] Hans-Georg Müller and Jane-Ling Wang. Hazard rate estimation under random censoring with varying kernels and bandwidths. *Biometrics*, 50(1):61–76, 1994.

SUPPORTING INFORMATION

None.



APPENDIX

In this section, we present some key theoretical results that lay the foundation of the methods in Section 2. Recall that in Section 2, we present a three-step method to select $h = \hat{h}(K_o)$ as the final bandwidth parameter in the estimation (2). Theorem 1 stated that $\hat{h}(K_o)$ is asymptotically equal to the optimal bandwidth h^* which minimizes MISE. To prove this, several key results are

leading to the theorem. We introduce the mean average square error defined as follows:

$$\text{MASE}(h, K) = \mathbb{E} \left[\frac{1}{n} \sum_{i=1}^n (\mu(\mathbf{X}_i) - \hat{\mu}_{h,K}(\mathbf{X}_i))^2 \mid \mathbf{X} \right],$$

where h is the bandwidth and K represents the kernel function. MASE is a mathematical approximation for the integrate MISE. Next, we show that with kernel function K_z , we can remove the correlation structure.

Theorem A.1. *Suppose model (1) and assumptions A1-A3 holds, the kernel function K_z satisfies C1 to C3 with non-zero support on an annular regions $c_1 < \|\mathbf{u}\| < c_2$ and the bandwidth $h \in (a_1 n^{-\frac{\alpha}{D+4}}, a_2 n^{-\frac{\alpha}{D+4}})$ for some positive numbers a_1 and a_2 , then there exist c_1 such that*

$$\text{MASE}(h, K_z) = \mathbb{E} [\text{RSS}(h, K_z) \mid \mathbf{X}] - \sigma^2 + o_p \left(\frac{1}{n^\alpha h^D} \right).$$

Corollary A.1. *Suppose that conditions in Theorem A.1 are satisfied. Then*

$$\text{MISE}(h, K_z) = \mathbb{E}[\text{RSS}(h, K_z) \mid \mathbf{X}] - \sigma^2 + o_p \left(\frac{1}{n^\alpha h^D} \right). \quad (\text{A.1})$$

Corollary A.1 indicates that with the kernel function K_z , we can remove the error correlation effect for bandwidth selection. We emphasize that this is not generally true with other kernel functions. For the bimodal kernel with only $K(0) = 0$, under assumptions A1 to A3, the result of (A.1) does not hold. The analysis is present in the S2.2 Remark of Supplementary.

Theorem A.2. *Suppose model (1) and assumptions A1-A3 hold, the kernel function K has bounded support and the bandwidth $h \in (a_1 n^{-\frac{\alpha}{D+4}}, a_2 n^{-\frac{\alpha}{D+4}})$ for some positive numbers a_1 and a_2 , then*

$$\text{Var}(\text{RSS}(h, K) \mid \mathbf{X}) = O_p(n^{-\frac{4\alpha}{D+4}}).$$

From Theorem A.2, we see that the conditional variance of $\text{RSS}(h, K_z)$ is bounded by the order of $n^{-\frac{4\alpha}{D+4}}$. Based on Corollary A.1 and Theorem A.2, it can be shown that the bandwidth minimize $\text{RSS}(h, K_z)$ will asymptotically minimize $\text{MISE}(h, K_z)$. Next, we establish the MISE of local linear regression estimator from bias and variance decomposition under the assumptions A1 to A3.

Theorem A.3. *Suppose model (1) and assumptions A1-A3 holds, the bandwidth satisfies $h \rightarrow 0$ and $n^\alpha h^D \rightarrow \infty$ as $n \rightarrow \infty$, then*

$$\text{MISE}(h, K) = \begin{cases} \frac{1}{4} h^4 \Delta_f^2 \mu_2(K)^2 + \frac{\sigma^2 (C_\rho + m(\mathcal{X}))}{n h^D} \mu(K^2) + o_p \left(h^4 + \frac{1}{n h^D} \right), & \alpha = 1, \\ \frac{1}{4} h^4 \Delta_f^2 \mu_2(K)^2 + \frac{\sigma^2 C_\rho}{n^\alpha h^D} \mu(K^2) + o_p \left(h^4 + \frac{1}{n^\alpha h^D} \right), & 0 < \alpha < 1. \end{cases} \quad (\text{A.2})$$

From Theorem A.3, the asymptotic optimal bandwidth for a given kernel function K can be derived directly by minimizing the leading term of MISE in (A.2).

Corollary A.2. *Suppose that conditions in Theorem A.3 are satisfied, the bandwidth minimize leading term of $\text{MISE}(h, K)$ is*

$$h_{\text{opt}}(K) = \begin{cases} \left(\frac{4\sigma^2 (C_\rho + m(\Omega))}{\Delta_f^2} \frac{\mu(K^2)}{\mu_2(K)^2} \right)^{\frac{1}{D+4}} n^{-\frac{1}{D+4}}, & \alpha = 1, \\ \left(\frac{4\sigma^2 C_\rho}{\Delta_f^2} \frac{\mu(K^2)}{\mu_2(K)^2} \right)^{\frac{1}{D+4}} n^{-\frac{\alpha}{D+4}}, & 0 < \alpha < 1. \end{cases}$$

Suppose $h_{\text{opt}}(K_o)$ and $h_{\text{opt}}(K_z)$ are the bandwidth from (A.2) with kernel function K_o and K_z respectively, then the factor relation gives

$$h_{\text{opt}}(K_o) = h_{\text{opt}}(K_z) \left(\frac{\mu(K_o^2) \mu_2(K_z)^2}{\mu_2(K_o)^2 \mu(K_z^2)} \right)^{\frac{1}{D+4}}.$$